Opto-Electronic Advances

Original Article
2019, Vol. 2, No. 8

DOI: 10.29026/oea.2019.190012

Spectrum evolution of Rayleigh backscattering in one-dimensional waveguide

Fuhui Li[1], Tianyi Lan[1], Ligang Huang[1], Iroegbu Paul Ikechukwu[1], Wuming Liu[2] and Tao Zhu[1]*

Despite the tremendous awareness of Rayleigh scattering characteristics and its considerable research interest for numerous fields, no report has been documented on the dynamic characteristics of spectrum evolution (SpE) and physical law for Rayleigh scattering from a micro perspective. Herein, the dynamic characteristics of the SpE of Rayleigh scattering in a one-dimensional waveguide (ODW) is investigated based on the quantum theory and a SpE-model of Rayleigh backscattering (RBS) source is established. By means of simulation, the evolution law which represents the dynamic process of the spectrum linewidth at a state of continuous scattering is revealed, which is consistent with our previous experimental observation. Moreover, an approximate theoretical prediction of the existing relationship between the spectrum linewidth of RBS source and the transmission length in ODW is proposed, which theoretically provides the feasibility of constructing functional devices suitable to ascertain laser linewidth compression. The designed experimental scheme can be implemented provided the assumptions are fulfilled. In addition, a theoretical model of the micro-cavity structure to realize the deep compression of laser linewidth is proposed.

Keywords: scattering; Rayleigh; spectrum evolution; linewidth; functional device

Li F H, Lan T Y, Huang L G, Ikechukwu I P, Liu W M *et al*. Spectrum evolution of Rayleigh scattering in one-dimensional waveguide. *Opto-Electron Adv* **2**, 190012 (2019).

Introduction

Rayleigh scattering mechanisms which consist of spontaneous Rayleigh scattering (SponRS) and stimulated Rayleigh scattering (STRS) have been tremendously investigated and widely employed in fundamental researches and potential applications[1,2]. The SponRS which has been greatly studied for its birefringence and polarization properties in the optical time-domain reflectometer and communications is mainly associated with the density fluctuations partly caused by local thermal fluctuations in mediums[3–5]. On the other hand, the STRS was observed in a linearly absorbing media and was attributed to light-induced localized thermal fluctuations[6–9]. In this process, STRS presents an unusual anti-Stokes frequency shift of approximately one half of the half intensity width of the pump laser. Despite the aforementioned devoted research efforts, the spectrum characteristics were not systematically investigated, which is an essential characteristic of Rayleigh scattering.

In our previous work, we investigated Rayleigh backscattering (RBS) in different types of optical fibers and some applications of Rayleigh scattering such as narrower filter, have be attained[10,11]. Moreover, we applied the characteristic of the RBS to the field of narrow linewidth lasers, precisely for attaining deep compression of the laser linewidth[12]. In this process, the spectrum evolution (SpE) characteristics of the RBS are the fundamental approach employed to realize a compressed laser linewidth. Despite significant research progress, previous analysis has primarily focused on the experimental results and macro-perspective. The microphysical processes and the dynamic characteristics of SpE for Rayleigh scattering are intriguing and greatly desirable, since ultimately numerous relevant experimental phenomena in practice require such theoretical analysis. It remains a challenge and almost unexplored area to comprehend such behavior in a microcosmic analysis for Rayleigh scattering.

[1]Key Laboratory of Optoelectronic Technology and Systems (Education Ministry of China), Chongqing University, Chongqing 400044, China; [2]Beijing National Laboratory for Condensed Matter Physics, Institute of Physics, Chinese Academy of Sciences, Beijing 100190, China.
*Correspondence: T Zhu, E-mail: zhutao@cqu.edu.cn
Received: 10 April 2019; Accepted: 28 June 2019; Published: 16 August 2019

In this paper, we have focused on the RBS and investigated the microscopic characteristics of SpE in a one-dimensional waveguide (ODW) based on the quantum theory. The dynamic process of the SpE is revealed in essence. According to the Jaynes-Cummings (J-C) model[13,14] and taking into account the system dissipation[15,16], we have established a SpE-model of RBS source in ODW and simulated the evolution process of spectral linewidth during the continuous scattering process, which is equivalent to a dynamic filtering model with a continuous narrowing linewidth. As a resultant of the continuous scattering for each scattering source amidst the transmission process, the spectrum linewidth of scattering field would decrease with the increase of the transmission length, and likewise weakly shrink to the short-wave direction relative to the initial pump field. On the basis of theoretical assumptions, we propose an approximate theoretical prediction that describes the relationship between the spectrum linewidth of the scattering field and the transmission length. This ultimately inspires the feasibility of constructing a micro-cavity structure capable of attaining linewidth compression theoretically, provided the scattering field could be separated and collected during continuous scattering. In accordance to the SpE characteristics and law of Rayleigh scattering in ODW, we also propose a theoretical model of the micro-cavity structure to realize the deep compression of laser linewidth.

Dynamic analysis model and simulation

The interaction Hamiltonian of electrons of scattering medium in the radiation field is described as[17–19]:

$$H_{\mathrm{er}}=\frac{e^2}{2m}\boldsymbol{A}\cdot\boldsymbol{A}-\frac{e}{m}\boldsymbol{p}\cdot\boldsymbol{A}\quad , \tag{1}$$

where m is the mass of the electron, e is the electron charge, $\boldsymbol{p}$ is the momentum operator of the electron, and $\boldsymbol{A}$ is the vector potential of the radiation field. The first group of mathematical symbols is called $\boldsymbol{A}^2$ term, which generally contributes to the matrix-element of light scattering. It involves the scattering of an even number of photons while the atomic states remain unchanged during the energy level transition. The second group of mathematical symbols is called the $\boldsymbol{p}\cdot\boldsymbol{A}$ cross term, which is a linear term in the expression of generation and annihilation operator of the photons. According to the microscopic characteristics of scattering, Rayleigh scattering is derived from the radiation field, and it belongs to the two-photon process involving the emission and absorption of photons. Only the $\boldsymbol{A}^2$ of the H_{er} contributes to it. The transition probability of Rayleigh scattering is described as Eq. (2) when the system changes from the initial state $|\phi_i\rangle=|\psi_i\rangle|n_1\rangle|n_2\rangle$ to the final state $|\phi_f\rangle=|\psi_i\rangle|n_1-1\rangle|n_2+1\rangle$.

$$P=|\langle\phi_{\mathrm{f}}|S|\phi_i\rangle|^2\quad , \tag{2}$$

where S is the scattering operator handled by second-order approximation, $|\psi_i\rangle$ represents the atomic state, $|n_1\rangle$ and $|n_2\rangle$ represent the photon number states of the pump field and the scattered field, respectively. If other components of the radiation field are ignored, equation (2) suggests the Rayleigh scattering would occur provided the system changes from the initial state $|\phi_i\rangle$ to the final state $|\phi_f\rangle$. Thus, pump field will be at the $|n_1-1\rangle$ whereas the scattered field is at the $|n_2+1\rangle$, which connotes the larger the transition probability of the absorption and radiation, the higher the Rayleigh scattering intensity. In ODW, the RBS will be accumulated along the ODW length.

Based on the J-C model and the consideration of dissipation[13–16], the single mode light field is a multi-frequency field with a specific linewidth and continuous distribution in the frequency domain. As shown in Fig. 1, the spectrum analysis of Rayleigh scattering can be divided into two steps namely: the generation of the RBS sources along the ODW during the forward transmission of pump field and the continuous scattering process of each RBS source during the backward transmission. For the aim of a convenient analysis, a unit cell on the cross section of the ODW can be regarded as a distributed scattering point. The initial seed source of Rayleigh scattering at each distributed scattering point will emerge due to the interaction between the pump field and waveguide cross-section atom. In this process, although the scattering generated in a waveguide is a distributed scattering with multiple directions, we investigated its evolution characteristics of the spectrum linewidth by the backscattering in ODW, and the enlarged figure represents a unit cell structure. Assuming the ODW consists of the same unit cell, each RBS source generated by a continuous pump field at every distributed point will be regarded as the same. According to Eq. (3), the radiative transition probability of a single atom from an up energy state $|i\rangle$ to a low energy state $|j\rangle$ can be expressed as[20–22]:

$$P=\frac{4\pi^2c^2}{3\hbar^2\omega}\left|\langle i|\frac{e}{mc}\boldsymbol{p}\,\mathrm{e}^{-\mathrm{i}\boldsymbol{k}\cdot\boldsymbol{r}}|j\rangle\right|^2\rho(\omega)\quad , \tag{3}$$

where $\rho(\omega)$ is the energy density of unit frequency, when the $\mathrm{e}^{-\mathrm{i}\boldsymbol{k}\cdot\boldsymbol{r}}$ of Eq. (3) is replaced by $\mathrm{e}^{\mathrm{i}\boldsymbol{k}\cdot\boldsymbol{r}}$, P is used to describe the absorption transition probability. Since P is directly proportional to the $\rho(\omega)$, the intensity distribution of each RBS source at each distributed point will slightly tend to the high-frequency part in comparison to the initial pump field. It is evident that the intensity of Rayleigh scattering will increase with the increase of the transmission length due to the accumulation of RBS sources along ODW. Moreover, we select the kth RBS source as a representative to investigate the SpE law of each RBS source during the continuous scattering process. The inset picture in Fig. 1 shows the separation and collection of each RBS field during the continuous scattering of the kth source via an optical circulator (OC), whereas the red pellet represents the multiple distributed scattering point in ODW. According to the transition characteristics presented in Eq. (3), the spectrum of the RBS field will weakly shrink to the short-wave direction with the increase of transmission length during the continuous scattering process. It is evident that the SpE characteristic of the Rayleigh scattering in ODW is mainly attributed to the continuous scattering process of each scattering source. As a resultant of a continuous incident pumped field, the SpE characteristic of the Rayleigh scattering in ODW would synthesize the statistical characteristics of each scattering source.

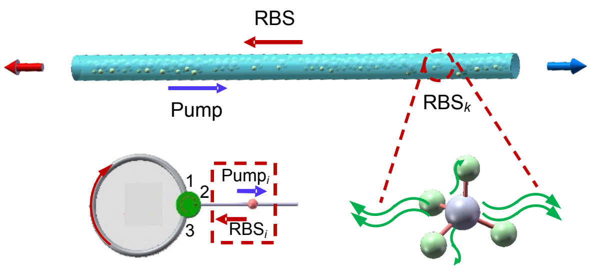

Fig. 1 | Schematic diagram of Rayleigh scattering spectrum analysis in an ODW. The inset picture represents the separation and collection of each RBS field during the continuous scattering process.

In the evolution process of quantum system discussed above, isolated system is mostly considered. However, in practical process, the system we investigated inevitably interacts with the surrounding environment. In addition, the scattering of light field in a waveguide device is a complicated process. Apart from Rayleigh scattering, there exist other forms of scattering including: Brillouin scattering and Raman scattering. Also, there are some other influencing factors, such as imperfections in the waveguide causing loss, coupling to free-space mode and cooperative effects in scattering. Herein, we have neglected the influence of other factors and mainly focused on the RBS to reveal the SpE characteristics of Rayleigh scattering in dissipative system. Generally speaking, there are many methods to deal with dissipative quantum theory[23–26], such as quantum trajectory method and input-output theory. Based on the frequency distribution characteristics of light field under the consideration of dissipation, which is a multi-frequency field with a specific linewidth and continuous distribution in the frequency domain, the reservoir can be regarded as a set of harmonic oscillators with continuous frequency distribution. Also, the effect of reservoir on the cavity field is expressed in the form of equivalent input and output fields.

By discussing the relationship among internal cavity field, input field and output field during the continuous scattering process, an analytical evolution model of the kth RBS source is established to describe the physical process of SpE in ODW intuitively. In this process, each scattering field in the continuous scattering process is employed to act as an internal cavity field. And the output field in the previous scattering is employed to act as an input field corresponding to the next scattering. Ultimately the SpE law of each RBS source during continuous scattering is equivalent to a dynamic filtering model with a continuous narrowing linewidth in frequency domain. The power spectrum after cycle for i times can be expressed as[23,24]:

$$S^{i}_{\mathrm{RBS}k}(\omega)=\{[\frac{\gamma_i}{\gamma_i-i(\omega-\omega_i)}]\cdot[\frac{\gamma_{i-1}}{\gamma_{i-1}-i(\omega-\omega_{i-1})}]\cdots [\frac{\gamma_1}{\gamma_1-i(\omega-\omega_1)}]\}\cdot S_0(\omega) \quad , \tag{4}$$

where γ_i is half the linewidth of the ith filtering model, ω_i is the center frequency of the ith filtering model. Based on the continuous narrowing characteristic in frequency domain of the analysis model, the γ_i can be expressed as $\gamma_i=\gamma_1 e^{-\beta i}$, where β represents Rayleigh scattering coefficient of waveguide material. Although each scattering field varies within the spectral range of the initial incident light field during the continuous scattering process, the radiation transition probability P is related to the unit energy density according to the microscopic physical process. In order to characterize the difference of each scattering field during the continuous scattering process, we introduce a density constant k to approximate the ω_i as:

$$\omega_i=[1+\frac{\rho_i(\omega)}{k}]\omega_{i-1} \quad , \tag{5}$$

where $\rho_i(\omega)$ represents the unit energy density of the power spectrum after ith filtering, k is used to characterize the energy density corresponding to the natural transition frequency ω_{a0} of atoms in a waveguide medium, which can be regarded as a constant value for a given waveguide medium. And there exists $\rho_i(\omega) << k$ under the same condition. $S_0(\omega)$ is the initial pump field injected into the ODW expressed as:

$$S_0(\omega)=\frac{\langle n\rangle}{\pi}\frac{\gamma/2}{(\omega-\omega_0)^2+(\gamma/2)^2} \quad , \tag{6}$$

where $\langle n\rangle$ represents the average number of photons of $S_0(\omega)$, γ is the linewidth and ω_0 is the center frequency. Based on the continuous narrowing characteristic of the frequency linewidth of the analysis model, Rayleigh scattering can be employed to act as an effective mechanism to produce a weak signal with continuous narrowing in frequency domain. In addition, the characteristics of the SpE of Rayleigh scattering in ODW become a statistical effect for each RBS source in the actual process, which is consistent with our previous experimental observation[10].

According to Eq. (4), the SpE-dynamic process of the kth RBS source during the continuous scattering process is shown in Fig. 2(a). In the simulation, the 3-dB linewidth of the initial pump light with Lorentzian line shape is set to be 2 MHz, γ_1 is set to be 1 MHz. Due to $v=\omega/2\pi$, the frequency corresponding to the central wavelength can be described by v_0. Herein, the span is set to be 6 MHz, which means the value of Δv is 1 MHz in

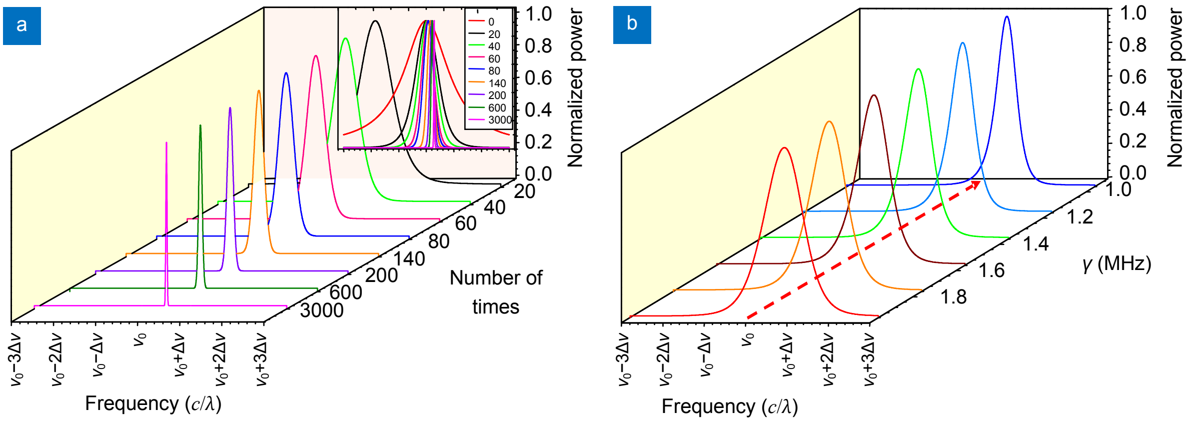

Fig. 2 | Simulation of the SpE law for the *k*th RBS source in the continuous scattering process. (**a**) The frequency spectra of the *k*th RBS source at different filtering number of times; (**b**) The frequency spectra of the *k*th RBS source under different effective dopant degree (EDD).

the simulation. In order to conveniently execute the simulation, $\rho_i(\omega)/k$ is set to be 0.0001, which characterizes the statistical value of v_i in the continuous scattering process[27]. Curves of different colors represent the normalized power spectra of the *k*th RBS source at various filtering number. To describe the fundamental law of the SpE of each RBS source clearly, a small illustration is introduced in Fig. 2(a). The red curve is the normalized power spectrum of the $S_0(\omega)$. It is evident that the linewidth of the normalized power spectrum undergoes a decrease in correlation to an increase in the number of cycles. In comparison to the $S_0(\omega)$, the spectra of the RBS source weakly shrinks to the short wave direction during the continuous scattering process. Likewise, the effect of an effective doping degree (EDD) on the SpE of the *k*th RBS source is investigated when the number of filtering is set to be 20, as shown in Fig. 2(b). Here, the EDD is used to characterize the reasonable auxiliary energy-level in the system, and the impact of the EDD is equivalent to changing the linewidth of the SpE-model. In the simulation, we can use the linewidth reduction of the SpE-model to characterize the increase of the EDD. The red dotted arrow in Fig. 2(b) represents the SpE direction with the increase of the EDD. It is observable that the linewidth of the spectra would undergo a decrease in correlation to an increase of the EDD. This can support the reason for the choice of inhomogeneous fiber employed as the RBS fiber in a narrow linewidth laser system[11].

Approximate theoretical prediction

According to the physical theory of the SpE-model, the decay of the internal cavity field is a crucial factor of the SpE of each RBS source amidst the continuous scattering process. Based on the quantum jump theory[28,29], with a focus on the decay of average photon number of the internal cavity field, an approximate theoretical prediction to describe the relationship between the SpE of each RBS source and the transmission length is proposed in ODW provided the waveguide material is determined. The relational expression which exists between the number of the cycles and the effective transmission length can be approximated as:

$$L=\sum_{i=1}^{N}L_i=\sum_{i=1}^{N}\frac{<n_0>_i\, l_{0i}}{n_0}\ , \tag{7}$$

where N is the number of the cycles, $\langle n_0\rangle_i$ is the average photon number attenuated in the ith cycle, l_{0i} is the coherence length of the scattering field after ith cycle, which is used to approximately characterize the effective length corresponding to photon annihilation, and n_0 is the effective number of single-electron atoms distributing on the cross-section of the ODW. According to Eq. (7) and Fig. 2, the relationship between the SpE of each RBS source and L would be established. In order to conveniently execute the simulation, the parameters are set as follows: $n_0=10\langle n_0\rangle_i$, and $l_0=150$ m, which corresponds to the coherence length of the $S_0(\omega)$ with a linewidth of 2 MHz. As shown in Fig. 3, the black square curve reveals a changed relationship between the SpE of the ith RBS source and the L amidst the continuous scattering in ODW. It can be observed that the spectrum linewidth of each RBS source will decrease with an increase of the L. The blue curve

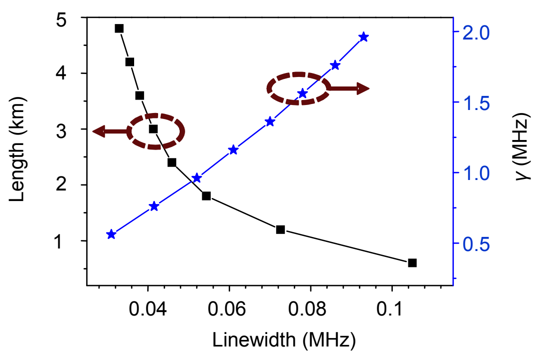

Fig. 3 | Theoretical prediction: the black curve with square describes the relationship between the spectral linewidth of the *k*th RBS source and the transmission distance *L*, while the blue curve with five-pointed star reveals the relationship between the spectral linewidth of the *k*th RBS source and the effective dopant degree (EDD).

with five-pointed star reflects the effect of the EDD on the SpE of the RBS source during the continuous scattering process, which is corresponding to Fig. 2(b). And it means that the spectrum linewidth of each RBS source will decrease with an increase of the EDD.

It is worth noting that the actual value of the SpE rate of each RBS source would be less than the theoretical predicted value as a consequence of the decay rate of the photon within the internal cavity field being relatively lesser than it's decoherence rate. In comparison to the traditional optical feedback method employed to narrow laser linewidth mainly by increasing the cavity length, the RBS method acting as a new mechanism can provide a weak optical feedback signal with a continuous narrowing linewidth in frequency domain during laser oscillation, which is the core of realizing the deep compression of laser linewidth. Therefore, the fundamental SpE law revealed in the theoretical prediction would offer the feasibility of constructing a functional device capable enough to attain linewidth compression in the field of narrow linewidth lasers theoretically. In this process, the RBS signal can be accumulated by designing a special waveguide structure and a micro-cavity structure of realizing linewidth compression can be obtained by means of integrating techniques of material. Consistent with the aforementioned assumption, we can approximately predict the corresponding linewidth by the useful parameters (L, EDD) of a functional device, and equally combine the macro-structure optimization of the device with the micro-mechanism to construct an ameliorate functional device to attain the expected output linewidth theoretically, provided the constraints are ignored.

Experimental scheme and design of microcavity structure

In this section, we will introduce the experimental scheme employed to actualize the SpE law revealed by the proposed analysis model. Also, based on the SpE characteristic, we propose a theoretical design of micro-cavity structure feasible enough to attain deep laser linewidth compression.

Experimental scheme

Under normal circumstances, it is arduous to directly observe the dynamic physical process of the SpE of Rayleigh scattering. Based on our long-term research on fiber waveguide, we design an experimental scheme as shown in Fig. 4. A distributed feedback (DFB) laser with a certain linewidth acting as a pump light is injected into a non-uniform fiber via the port 2 of OC_1. Furthermore, the RBS_1 signal and the pump signal will be separated, and the RBS_1 signal originating from the port 3 of the OC_1 will be measured via the 10% output (Point A) of Coupler 1 (C_1). Whereas, the remaining light signal from the 90% output acting as a new pump light is injected into another non-uniform fiber via the port 2 of the OC_2 after being amplified by an erbium doped fiber amplifier (EDFA). Similarly, the RBS_2 signal generated from the RBS fiber will be measured via the 10% output (Point B) of Coupler 2 (C_2). Propagating across a series of sequences of the scattering system (SS), the RBS_n signal will be measured via the 10% output (Point N) of Coupler n. The linewidth of the RBS signal can be measured by a self-heterodyne detection system.

In this process, suppose i) the Rayleigh scattering coefficient of the non-uniform fiber used in the system is large enough; ii) the intrinsic linewidth remains unchanged when the RBS signal amplified by the EDFA has a sufficient power to act as the new pump light, the experimental scheme can be implemented. The part which consists of an OC_1 and C_1 in Fig. 4 has been implemented in our previous research[10]. During the experimental process, a fiber laser with a linewidth of 11.2 kHz acts as a pump light, and the linewidth of the RBS signal in three different types of fibers namely 2 km single mode fiber (SMF-28e), 7 km large effective area fiber (LEAF) and 100 m polarization maintaining fiber (PMS) are ~9 kHz, ~10 kHz, and ~11 kHz, respectively. According to our previous experimental results which is inclusive of the threshold power and the effective input power range for Rayleigh scattering, the power of the RBS source amplified by the EDFA can be set to be 17 dBm, 10.8 dBm and 23.9 dBm to act as the new pump light for the SMF-28e,

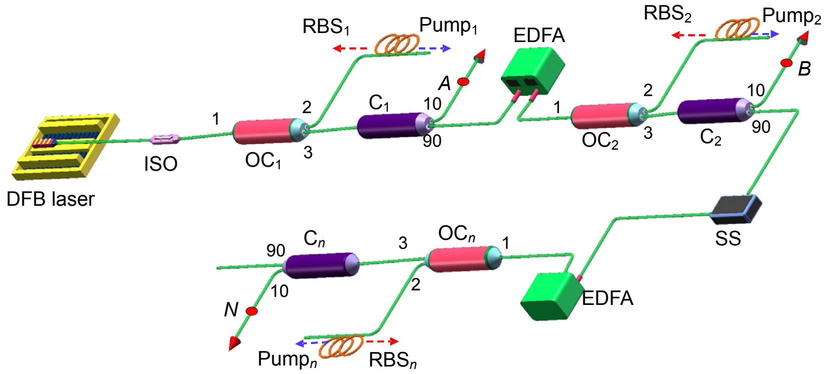

Fig. 4 | The experimental scheme for measuring the SpE of Rayleigh scattering. ISO: Optical isolator; OC: Optical circulator; C: 90:10 coupler; EDFA: Erbium doped fiber amplifier. SS: A series of sequences of the scattering system.

LEAF, and PMF, respectively. Attributing to the quest for improvement effect of the laser linewidth, the RBS acting as an effective mechanism employed to attain deep linewidth compression has been widely used in fiber lasers[30,31] and semiconductor lasers[32,33].

Theoretical design of micro-cavity structure

For narrow linewidth lasers, the traditional optical feedback method acting as a common mechanism is employed to narrow laser linewidth mainly by increasing the cavity length. Whereas the RBS method is solemnly based on the feedback of an excitation signal with a continuous narrowing linewidth in frequency domain which ultimately happens to be more advantageous in comparison to the aforementioned traditional method. Therefore, a quest to design a RBS device capable enough to separate and accumulate the scattering signal during the operational state of the laser is of paramount importance. Based on the SpE characteristics and law of Rayleigh scattering in ODW, we propose a theoretical model of an in fiber micro-cavity structure for a fiber laser, as shown in Fig. 5. A fiber laser with a wide-band fiber Bragg grating (WB-FBG) and a narrow-band FBG (NB-FBG) is controlled by a temperature control device to realize a stable output. The NB-FBG has a peak reflectivity of 60% and a 3 dB bandwidth of 0.2 nm, whereas that of the WB-FBG is more than 95% with a 3 dB bandwidth of 0.3 nm. Both FBGs operates at a wavelength of 1550 nm. A micro-cavity structure matching the laser output wavelength is placed at the output of the fiber laser to accumulate and feedback the RBS signal effectively. In order to stabilize the resonant wavelength of the micro-cavity to the laser wavelength, another temperature control device is required. Ultimately, a model of ultra-narrow linewidth laser with micro-cavity is obtained. Compared with conventional laser system, the in-fiber micro-cavity structure employed to effectively accumulate RBS signal can eliminate the external disturbances caused by long RBS fiber in laser system, which will facilitate the development of a portable ultra-narrow linewidth fiber laser of profound stability provided the limitations of process technology is ignored. Assuming the functional device can be obtained,

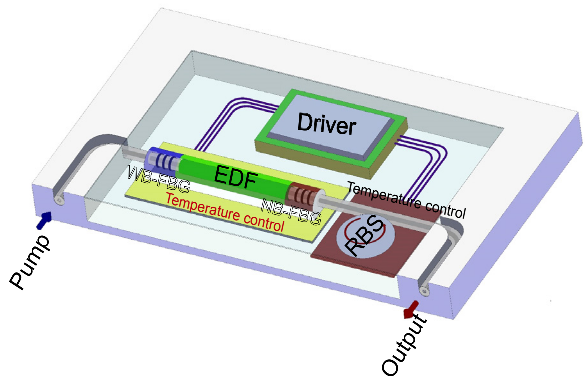

Fig. 5 | Theoretical design of micro-cavity structure based on the SpE characteristic of Rayleigh scattering in ODW.

and the output can be adequately controlled, this ultimately plays a vital role in the field of narrow linewidth laser. The output stability of the laser will be improved and the expected laser linewidth will be attained.

Discussion

Based on the dynamic analysis model with a continuous narrowing linewidth, Rayleigh scattering can be employed to act as an effective mechanism to realize a weak feedback signal with continuous narrowing in the frequency domain. Provided the micro-cavity structure based on this characteristic can be realized to sufficiently accumulate feedback signals, the large structure and complexity of the narrow linewidth laser system caused by the existence of a long RBS fiber will be eliminated. Ultimately, a portable ultra-narrow linewidth laser of profound stability would be realized. From a micro perspective, provided the relationship between the photon decay rate of internal cavity field and its decoherence rate can be quantitatively determined, the accuracy of our theoretical prediction can be further improved, which will greatly enhance the feasibility of constructing a micro-cavity structure of functional device in the field of narrow linewidth lasers. In a case scenario where limitations to the scientific-technological level and technical means do not exist, the optimization of the macro-structure of the device can be combined with the micro-mechanism to construct an ameliorative functional device, which will further enhance the development of narrow linewidth laser.

Conclusion

In summary, we have investigated the SpE characteristics of Rayleigh scattering in ODW based on the quantum theory. Attributable to the continuous scattering of each scattering source during the transmission process, the spectrum linewidth of scattering filed would decrease with the increase of the transmission length, and it would weakly shrink to the short-wave direction relative to the $S_0(\omega)$. According to the dissipative quantum theory, we have established a SpE-model of RBS during the continuous scattering process and simulated the evolution process of spectrum linewidth at different number of cycles. Moreover, based on the theoretical assumptions, we propose an approximate theoretical prediction for the relationship between the spectrum linewidth of the scattering field and the transmission length, which would offer the feasibility of constructing a functional device capable enough to attain linewidth compression theoretically, provided the scattering field could be separated and collected during the continuous scattering process. Ultimately, we have proposed a theoretical model of micro-cavity structure to realize a deep linewidth compression according to the SpE law of Rayleigh scattering in ODW. This theory provides a reference value and a theoretical support for the development of narrow linewidth lasers, which is also applicable in the theoretical design of micro-cavity structure of realizing the deep compression of laser linewidth.

References

1. Mizuno Y, Zou W W, He Z Y, Hotate K. Proposal of Brillouin optical correlation-domain reflectometry (BOCDR). *Opt Express* **16**, 12148–12153 (2008).
2. Maier R R J, Macpherson W N, Barton J S, McCulloch S, Jones B J S. Distributed sensing using Rayleigh scatter in polarization-maintaining fibres for transverse load sensing. *Meas Sci Technol* **21**, 094019 (2010).
3. Zhang Z Y, Bao X Y. Continuous and damped vibration detection based on fiber diversity detection sensor by Rayleigh backscattering. *J Lightw Technol* **26**, 832–838 (2008).
4. Pan Z Q, Yu C Y, Willner A E. Optical performance monitoring for the next generation optical communication networks. *Opt Fiber Technol* **16**, 20–45 (2010).
5. Zheng Y, Wu Z F, Shum P P, Xu Z L, Keiser G *et al*. Sensing and lasing applications of whispering gallery mode microresonators. *Opto-Electron Adv* **1**, 180015 (2018).
6. Faris G W, Markosyan A, Porter C L, Doshay S. Two-tone frequency-modulation stimulated Rayleigh spectroscopy. *Opt Lett* **39**, 4615–4618 (2014).
7. Dong L. Stimulated thermal Rayleigh scattering in optical fibers. *Opt Express* **21**, 2642–2656 (2013).
8. Cui J W, Dang H, Feng K P, Yang W L, Geng T *et al*. Stimulated Brillouin scattering evolution and suppression in an integrated stimulated thermal Rayleigh scattering-based fiber laser. *Photonics Res* **5**, 233–238 (2017).
9. He G S, Lu C G, Zheng Q D, Prasad P N, Zerom P *et al*. Stimulated Rayleigh-Bragg scattering in two-photon absorbing media. *Phys Rev A* **71**, 063810 (2005).
10. Zhu T, Bao X Y, Chen L, Liang H, Dong Y K. Experimental study on stimulated Rayleigh scattering in optical fibers. *Opt Express* **18**, 22958–22963 (2010).
11. Zhu T, Bao X Y, Chen L. A single longitudinal-mode tunable fiber ring laser based on stimulated Rayleigh scattering in a nonuniform optical fiber. *J Lightw Technol* **29**, 1802–1807 (2011).
12. Huang S H, Zhu T, Yin G L, Lan T Y, Huang L G *et al*. Tens of hertz narrow-linewidth laser based on stimulated Brillouin and Rayleigh scattering. *Opt Lett* **42**, 5286–5289 (2017).
13. Zheng S B. Jaynes-Cummings model with a collective atomic mode. *Phys Rev A* **77**, 045802 (2008).
14. Romanelli A. Generalized Jaynes-Cummings model as a quantum search algorithm. *Phys Rev A* **80**, 014302 (2009).
15. Peano V, Thorwart M. Quasienergy description of the driven Jaynes-Cummings model. *Phys Rev B* **82**, 155129 (2010).
16. Chen Q H, Liu T, Zhang Y Y, Wang K L. Exact solutions to the Jaynes-Cummings model without the rotating-wave approximation. *Europhys Lett* **96**, 14003 (2011).
17. Duan C K, Wen H L, Tanner P A. Local-field effect on the spontaneous radiative emission rate. *Phys Rev B* **83**, 245123 (2011).
18. Sharapova P R, Tikhonova O V. Coherent control of interaction and entanglement of a Rydberg atom with few photons. *Laser Phys Lett* **10**, 075204 (2013).
19. Cheung H K, Law C K. Optomechanical coupling between a moving dielectric sphere and radiation fields: a Lagrangian-Hamiltonian formalism. *Phys Rev A* **86**, 033807 (2012).
20. Li Z X, Yin C H. The ground-state transition probability of impurity bound polaron in quantum rod. *Phys B Condens Matter* **418**, 69–72 (2013).
21. Akbari M, Andrianov S N, Kalachev A A. Quantum logic gates based on off-resonant cavity-assisted interaction between three-level atoms and single photons. *Laser Phys* **27**, 075202 (2017).
22. Abdi M, Degenfeld-Schonburg P, Sameti M, Navarrete-Benlloch C, Hartmann M J. Dissipative optomechanical preparation of macroscopic quantum superposition states. *Phys Rev Lett* **116**, 233604 (2016).
23. Benito M, Mi X, Taylor J M, Petta J R, Burkard G. Input-output theory for spin-photon coupling in Si double quantum dots. *Phys Rev B* **96**, 235434 (2017).
24. Raymer M G, McKinstrie C J. Quantum input-output theory for optical cavities with arbitrary coupling strength: application to two-photon wave-packet shaping. *Phys Rev A* **88**, 043819 (2013).
25. Häyrynen T, Oksanen J, Tulkki J. Dynamics of cavity fields with dissipative and amplifying couplings through multiple quantum two-state systems. *Phys Rev A* **83**, 013801 (2011).
26. Naether U, Quijandría F, García-Ripoll J J, Zueco D. Stationary discrete solitons in a driven dissipative Bose-Hubbard chain. *Phys Rev A* **91**, 033823 (2015).
27. Shi J L, Wu H P, Yan F, Yang J J, He X D. Experimental study on stimulated scattering of ZnO nanospheres dispersed in water. *J Nanopart Res* **18**, 23 (2016).
28. Häyrynen T, Oksanen J, Tulkki J. Unified quantum jump superoperator for optical fields from the weak- to the strong-coupling limit. *Phys Rev A* **81**, 063804 (2010).
29. Gammelmark S, Mølmer K, Alt W, Kampschulte T, Meschede D. Hidden Markov model of atomic quantum jump dynamics in an optically probed cavity. *Phys Rev A* **89**, 043839 (2014).
30. Yin G L, Saxena B, Bao X Y. Tunable Er-doped fiber ring laser with single longitudinal mode operation based on Rayleigh backscattering in single mode fiber. *Opt Express* **19**, 25981–25989 (2011).
31. Pang M, Xie S R, Bao X Y, Zhou D P, Lu Y G *et al*. Rayleigh scattering-assisted narrow linewidth Brillouin lasing in cascaded fiber. *Opt Lett* **37**, 3129–3131 (2012).
32. Liang W, Ilchenko V S, Savchenkov A A, Matsko A B, Seidel D *et al*. Whispering-gallery-mode-resonator-based ultranarrow linewidth external-cavity semiconductor laser. *Opt Lett* **35**, 2822–2824 (2010).
33. Liang W, Ilchenko V S, Eliyahu D, Savchenkov A A, Matsko A B *et al*. Ultralow noise miniature external cavity semiconductor laser. *Nat Commun* **6**, 7371 (2015).

Acknowledgements

This work was supported by the Key Research and Development Project of Ministry of Science and Technology (2016YFC0801200), the National Natural Science Foundation of China (NSFC) (61635004), the National Science Fund for Distinguished Young Scholars (61825501). the National Key R&D Program of China (2016YFA0301500), NSFC (11434015, 61835013), the Strategic Priority Research Program of the Chinese Academy of Sciences (XDB01020300, XDB21030300).

Competing interests

The authors declare no competing financial interests.